

The effect of ZnO cupping layer on the formation of sol-gel synthesized Ag nanoparticles

L.A. Sokura ^{1,2}✉, A.V. Kremleva ², A.E. Romanov ¹⁻³

¹ Ioffe Institute, St. Petersburg, Russia

² ITMO University, St. Petersburg, Russia

³ Togliatti State University, Togliatti, Russia

✉ sokuraliliy@itmo.ru

Abstract. Samples containing Ag nanoparticles (NPs) in a ZnO matrix were produced using a sol-gel method, with varying the annealing temperature and the thickness of the ZnO cupping layer. The dependence of the optical and structural properties of the samples on the silver diffusion was studied. As a result of annealing at temperatures of 570-650 °C, a long-wavelength shift of the plasmon absorption peak of NPs was observed due to an increase in their average size, as well as an increase in the intensity of the absorption peak due to a narrower size distribution of NPs. The transformation of the nanoparticle shape and size during annealing was shown to result from the diffusion of silver, whereas the ZnO cupping layer and its thickness was proved to control these processes.

Keywords: Ag nanoparticles; zinc oxide; sol-gel synthesis; plasmonics; scanning electron microscopy; transmission electron microscopy

Acknowledgements. The work was carried out with the support of the Ministry of Science and Higher Education of the Russian Federation (agreement No 075-15-2021-1349).

Citation: Sokura LA, Kremleva AV, Romanov AE. The effect of ZnO cupping layer on the formation of sol-gel synthesized Ag nanoparticles. *Materials Physics and Mechanics*. 2023;51(4): 76-84. DOI: 10.18149/MPM.5142023_7.

Introduction

Uniform arrays of metal nanoparticles (NPs) embedded in a dielectric or semiconductor matrix have unique optical, catalytic, magnetic, electronic, and other properties, which are controlled by plasmonic phenomena. The mentioned properties depend on the composition, size, and shape of the particles, as well as on the distance between them. In recent years, the nanostructures comprised of NPs have been increasingly used as active elements for producing solid-state chemical and biological sensors [1,2], catalytic systems [3], optical devices and other applications [4,5]. Such systems require precise control of the NPs density in the array, also, a two-dimensional array structure with a well-defined geometry is to be formed on the substrate. The size of the NPs can influence the defective structure of the NPs [6–9], which is also important for their functional properties. Conventional methods, including ion implantation, chemical or vacuum deposition, do not appear to produce uniform NP arrays with narrow distributions of particle sizes and the distances between them [10–12]. Therefore, in recent years, various modifications of these methods were developed, for example, colloidal lithography [13], laser interference lithography [14], vapor phase deposition through a mask of a given pattern [15,16], adsorption of NPs from colloidal solutions onto substrates modified by

the self-organizing monolayers of functionalized silanes and thiols [17], microcontact printing [18].

Uniform NPs array fabrication requires a detailed study of their formation processes. Although multiple papers have been published on the topic, a clear physical model of metal NP formation process in a dielectric matrix does not seem to have been reported. However, the NP formation is known to result from sequential addition of metal atoms or ions to each other due to the activation of diffusion processes in the matrix [19–21]. Otherwise, two simultaneous processes of coalescence (the augmentation of the NP sizes and an increase in the distance between them) and evaporation are responsible for the formation of NPs during the thermal decomposition of Ag and Au thin films [22–24].

Our previous research involved experiments for producing silver NP arrays in thin ZnO films deposited on quartz substrates by sol-gel method [25–27]. We showed that the diffusion through annealing in such samples results in significant changes in the morphological and optical properties of the Ag NP arrays. At a fixed annealing time (10–15 minutes), an increase in the annealing temperature from 300 to 650 °C caused an increase in the NP size from 20–30 to 50–70 nm. With a further increase in the annealing temperature up to 700 °C, we observed NPs decomposition and diffusion of silver into the quartz substrate with the formation of small clusters up to 10 nm in diameter in the near-surface layer of the substrate [25]. Besides, there was an increase in the NPs size with an increase in the annealing time from 5 to 20 minutes at a fixed temperature [26]. On the other hand, an increase in the silver concentration in the initial solution, as well as an increase in the number of the solution layers deposited on a substrate, resulted in an increase in the NPs array density while maintaining their size [27].

This paper discusses the effect of the ZnO cupping layer and its thickness on the parameters of the NPs. We produced a series of the samples with the silver NP array in a ZnO matrix, differing in the thickness of the ZnO coat and the annealing temperature. It was suggested that if it is the diffusion of silver in the ZnO layer being influential in the NP array formation, then when the annealing temperature changes while there is no ZnO layer or when its thickness is different, the diffusion processes would occur differently, and the resulting NP arrays will have different optical and structural properties.

Methods

We chose the sol-gel method to produce experimental samples. To study the effect of the ZnO matrix on the diffusion of silver, a series of samples was made that differ from each other in the annealing temperature and the thickness of the ZnO cupping layer.

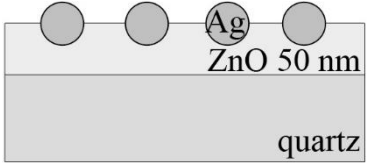
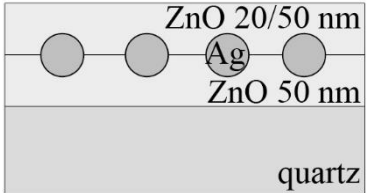
The solution for making Ag NPs contained silver nitrate (AgNO_3) in 2-Methoxyethanol ($\text{C}_3\text{H}_8\text{O}_2$) in the concentration of 0.05 M. The solution was treated on a magnetic stirrer for 10 minutes at a speed of 500 rpm at room temperature. No aging was required, so the solution was finished immediately before application.

The solution for producing the ZnO layers contained zinc acetate dihydrate ($\text{Zn}(\text{CH}_3\text{COO})_2 \cdot 2\text{H}_2\text{O}$) in the concentration of 0.2 M in 2-Methoxyethanol ($\text{C}_3\text{H}_8\text{O}_2$). To accelerate the sol aging, monoethanolamine ($\text{C}_2\text{H}_7\text{ON}$) was added to the solution in a ratio of 1:1 to Zn. The solution was treated on a magnetic stirrer for 60 minutes at a speed of 500 rpm at room temperature, then kept for 24 hours for aging and transition to the sol state.

The layers were coated on polished flat-parallel quartz plates by spin-coating method at a speed of 3500 rpm for 12 seconds. After coating, each layer was exposed to air drying for 3 minutes at 300 °C. To produce the samples for the experiment, the first 5 layers of the ZnO sol were deposited (equivalent to the 50 nm thick ZnO layer) followed by 5 layers of the silver nitrate solution. Further, more ZnO layers were applied on top with 0 (without ZnO coating), 2 or 5 layers of the ZnO sol. The resulting multilayer samples were not annealed, or else they were annealed in a muffle furnace in the air for 15 minutes at temperatures of 570 and 650 °C.

Thus, in total, 9 samples were prepared: without a ZnO cupping layer, with the ZnO cupping layer 20 and 50 nm thick (equivalent to the 2 and 5 ZnO spin-coated layers, respectively), without annealing or annealed at temperatures of 570 and 650 °C (Table 1).

Table 1. Description of produced samples

Sample layout	Sample №	Thickness of the ZnO cupping layer, nm	Annealing temperature, °C
	1	0	300
	2		570
	3		650
	4	20	300
	5		570
	6		650
	7	50	300
	8		570
	9		650

The optical absorption spectra of the samples were measured using an Avantes fiber-optic system based on the AvaSpec 2048 spectrometer and the AvaLight-DH-S-BAL radiation source, which provides measuring absorption and transmission spectra in the spectral range of 200–1100 nm.

The structural and morphological properties of the NP arrays in the samples produced were studied using a scanning electron microscope (SEM) Mira 3 Tescan and a transmission electron microscope (TEM) JEM-2100F JEOL. The combination of SEM and TEM methods provided a detailed study of the fabricated samples in the plan view and cross-section geometries.

Thin cross-section samples with Ag NPs in the ZnO matrix for TEM studies were prepared in accordance with the standard procedure, with preliminary mechanical thinning and subsequent polishing by an ion beam (Ar^+) with energy of 4 keV [28]. The TEM studies were performed using the equipment belonging to the Joint Research Center "Material science and characterization in advanced technology" (Ioffe Institute).

Results and Discussion

Figure 1 shows the absorption spectra of the samples containing Ag NP arrays in a ZnO matrix produced at different thicknesses of the ZnO cupping layer (0 nm – without a ZnO coating, 20 and 50 nm) and at different annealing temperatures (without annealing - after drying at 300 °C, annealing at 570 and 650 °C). Intense absorption at the wavelengths lower than 400 nm corresponds to the edge of the ZnO interband absorption [29].

Absorption peaks with different intensities in the range of 500–700 nm, observed in the samples, appear to be caused by the localized plasmon resonance in Ag NPs [30,31]. Parts (a) to (c) of Fig. 1 show that irrespective of the ZnO cupping layer thickness, the spectra behave similarly when annealing conditions change. After annealing at a temperature of 570 °C (samples № 2, 5, 8), the intensity of the NP absorption peak decreases and the peak widens compared to the sample without annealing (samples № 1, 4, 7). After annealing at a temperature of 650 °C (samples № 3, 6, 9), the intensity of the peak increases sharply, while the shape and the width of the peak remain unchanged.

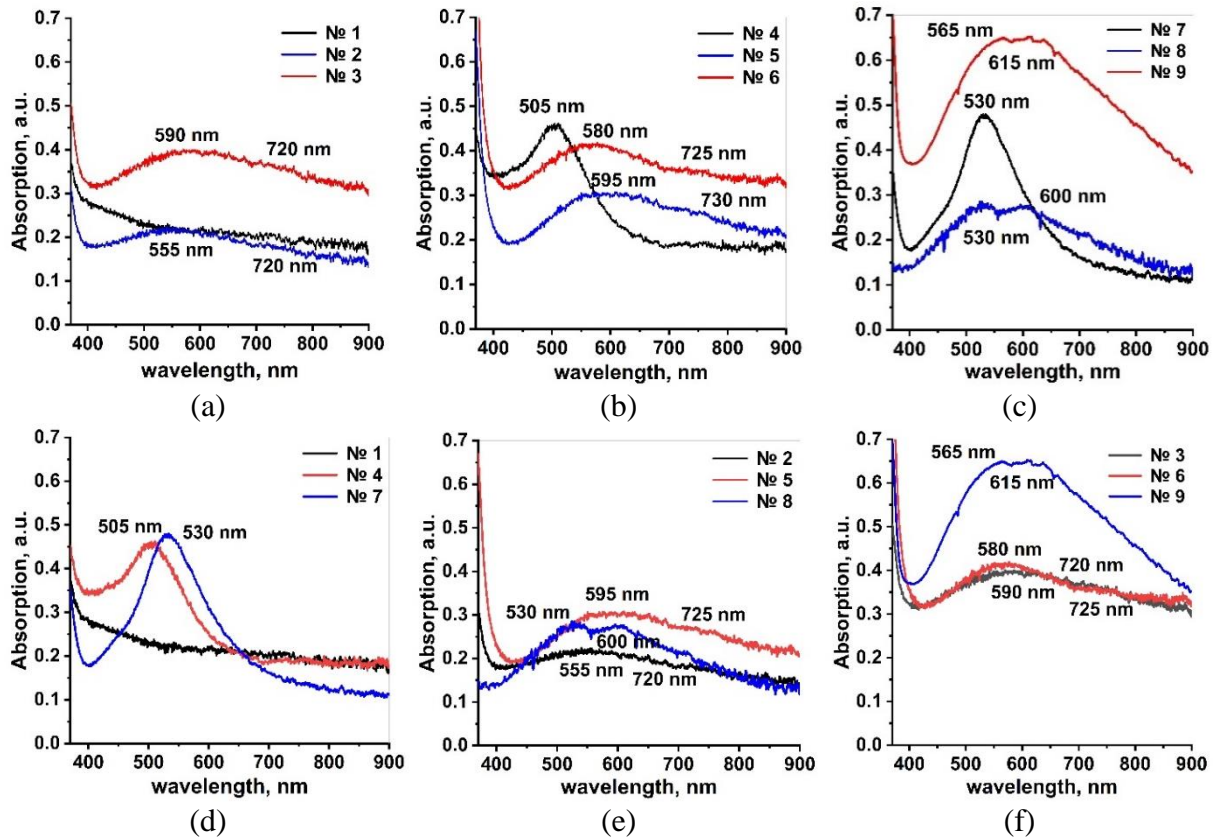


Fig. 1. Absorption spectra of the samples № 1 to 9 with Ag NPs in the ZnO matrix fabricated with different thicknesses of the ZnO cupping layer (0, 20 and 50 nm) and at different annealing temperatures (without annealing, annealing at 570 and 650 °C): (a) to (c) give a comparison based on the effect of annealing temperature at the same thickness of the ZnO cupping layer, (d) to (f) provide a comparison based on the effect of ZnO coat thickness at the same annealing temperature

Comparison of the spectra in parts (d) to (f) of Fig. 1 shows that ZnO cupping layer and its thickness have negligible effect on the shape and the spectral position of NP plasmon absorption peak. However, the addition of the ZnO cupping layer increases the absorption intensity of the NPs, which is especially noticeable for the samples without annealing (samples № 4, 7) and those annealed at 650 °C (samples № 6, 9). In the samples without a cupping layer of ZnO, the NP absorption peak has very low intensity, and in the sample without annealing, there is no peak at all (sample № 1).

The wavelength values corresponding to the spectral position of the NP absorption peak in the studied samples are marked with respective numbers in Fig. 1. In all samples annealed at 650 °C, the spectral position of the absorption peak is shifted to the long-wavelength region compared to the samples without annealing. In accordance with the theory of Mie [32], which describes the dependence of optical properties on the metal NP size, the shift of the absorption peak to the long-wavelength region indicates that the NP average size in the samples has increased as a result of annealing. All absorption spectra of the samples annealed at 570 and 650 °C are shown to have a long-wavelength shoulder in the range of 600–730 nm, in addition to the absorption peak in the range of 530–590 nm. They may represent a superposition of the absorption spectra of the array of NPs with varying sizes. Moreover, an additional peak appearing as a long-wavelength shoulder of the absorption spectrum, may indicate the possible non-sphericity of the NPs [33], for example, the NPs may become ellipsoidal or elongated in one or more directions.

A combined study of the sample structural properties by SEM and TEM methods detected the presence of two simultaneously existing entries: arrays of silver small NPs and large Ag submicroscopic particles (SMPs). Parts (a) to (c) of Fig. 2 show SEM images of the sample surface with no ZnO capping layer without annealing (sample № 1) and after it (samples № 2, 3). The images show that immediately after drying at 300 °C (without annealing, sample № 1), a NP array with a high density up to $1.5 \times 10^9 \text{ cm}^{-2}$ is formed, however, this array has a wide NP size distribution – some NPs with a diameter of 50 to 200 nm are observed, as well as some larger Ag SMPs reaching 500 nm in diameter. It is possible that the observed wide NP size distribution in this sample is responsible for a high absorption level in the whole visible spectrum range and the absence of an obvious NP absorption peak, see Fig. 1(a).

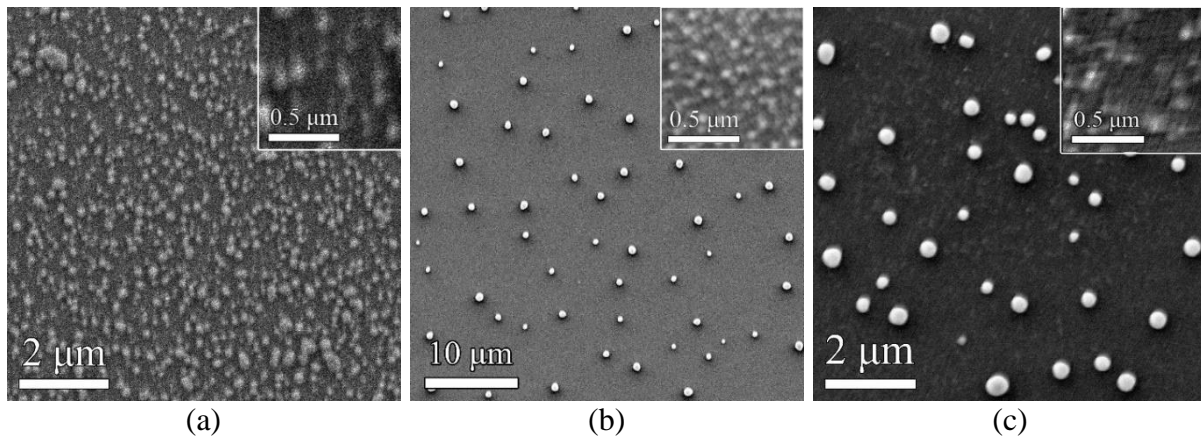


Fig. 2. SEM images of the surfaces samples № 1 to 3 with Ag particles without a ZnO capping layer produced by sol-gel method: (a) sample № 1 - without annealing, (b) sample № 2 - after annealing at a temperature of 570 °C and (c) sample № 3 - after annealing at a temperature of 650 °C. The inserts show magnified images of NPs

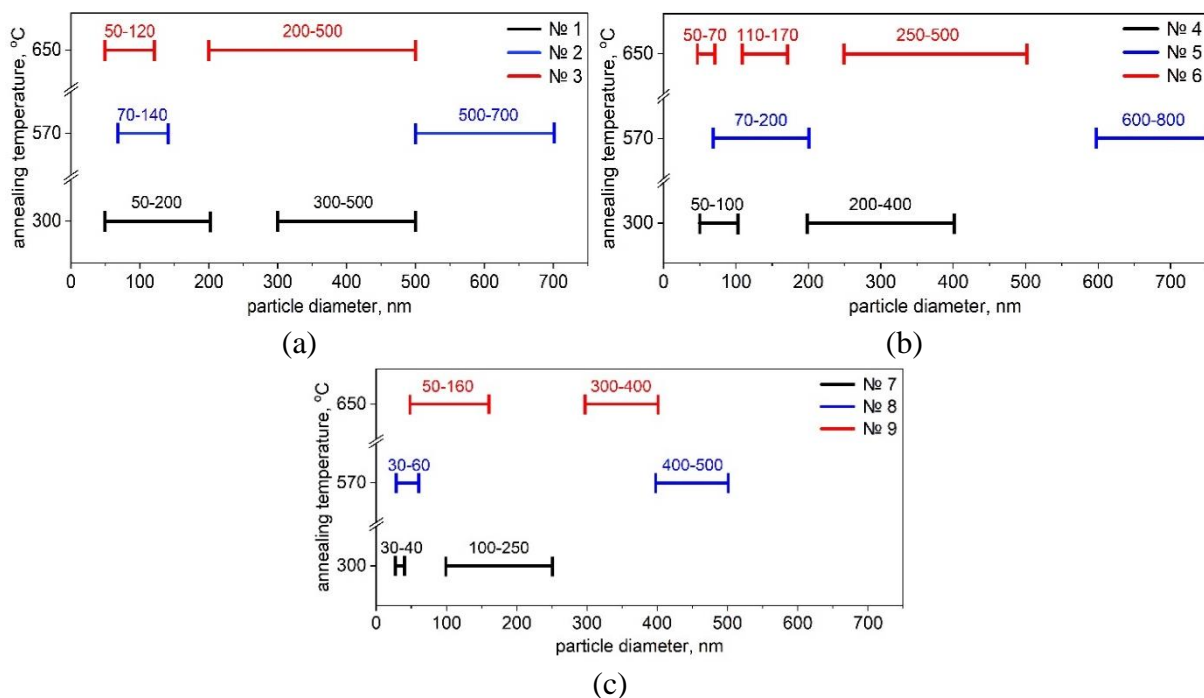


Fig. 3. Particle size distribution revealed by SEM and TEM studies in the samples № 1 to 9 without annealing (300 °C) and after annealing at temperatures of 570 and 650 °C: (a) samples № 1 to 3 - without a ZnO capping layer, (b) samples № 4 to 6 – covered with a 20 nm thin ZnO layer and (c) samples № 7 to 9 - covered with a 50 nm thick ZnO layer

As a result of annealing at the temperature of 570 °C (sample № 2), the NPs start being located more uniformly on the substrate surface, see Fig. 2(b). Besides the equidistant distribution of NPs in the array, they also demonstrate a narrower size distribution. In addition to a homogeneous array of ordered large SMPs with a diameter of 500-700 nm, some smaller NPs with a diameter of 70 to 140 nm are also observed in the sample. The number of the large SMPs compared to those in the sample before annealing has decreased by 2 orders - from 3×10^8 to 3×10^6 cm⁻², and the number of small NPs has increased to 8×10^9 cm⁻². Annealing at a temperature of 650 °C (sample № 3) has further decreased the particle size and distribution in arrays – the NP size ranged from 50 to 120 nm, large SMPs – from 300 to 500 nm, while the number of large SMPs has significantly decreased, see Fig. 2(b). For a sake of clarity, the particle sizes in the samples revealed by the results of SEM and TEM studies are shown in the graphs in Fig. 3.

The NP sizes in the samples covered with the ZnO layers demonstrated the changes in Ag NP distributions due to the effect of annealing in a similar way to the NP arrays in the samples without a ZnO cupping layer, see Figs. 3 and 4. First, the average particle size increases as a result of annealing at the temperature of 570 °C (samples № 5 and 8), and after annealing at 650 °C (samples № 6 and 9), it decreases. The addition of the ZnO cupping layer is shown to result in the narrowing of the NP size distribution, and to the reduction of the number and the size of large SMPs in the samples in the case of the largest thickness of the ZnO coating cupping layer (50 nm, samples № 8 and 9). Consequently, it can be concluded that large SMPs are formed during the coagulation of silver, whereas the ZnO cupping layer prevents this.

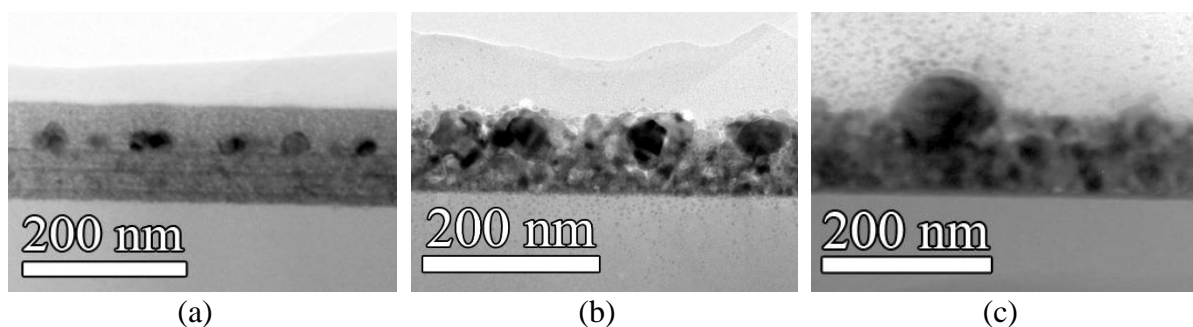


Fig. 4. TEM images of the samples № 7 to 9 with Ag particles with a 50 nm thick ZnO cupping layer produced by sol-gel method: (a) № 7 - without annealing, (b) № 8 - after annealing at a temperature of 570 °C and (c) № 9 - after annealing at a temperature of 650 °C

The sample absorption spectra suggested that the particle size should increase during the annealing process. This assumption is in good agreement with the data obtained from the studies of morphological and structural properties of the samples. The NP average size increased as a result of annealing, however, the size distribution narrowed, which contributed to an increase in the intensity of absorption peaks. An array of larger SMPs observed in the samples might be responsible for the appearance of long-wavelength shoulders in the range of 600–730 nm.

Since the amount of silver deposited is the same in all samples, it is the presence of the ZnO cupping layer that is responsible for the particle size change and the shift of the absorption peak. Referring to the earlier assumption that the transformation of the particle shape and size during annealing occurs due to silver diffusion [25,34], the fact is that the ZnO cupping layer and its thickness affect Ag diffusion to these processes.

Conclusion

Experiments have been conducted to study optical and structural properties of the samples with Ag NPs in a ZnO matrix made by the sol-gel method with different annealing temperature and thickness of the ZnO cupping layer. The absorption spectra of the produced samples did contain Ag NP plasmon absorption peak in the range of 500-700 nm. As a result of annealing at the temperature of 570-650 °C, a long-wavelength shift of the plasmon absorption peak was observed resulting from an increase in the NP average size, as well as an increase in the peak intensity resulting from the narrowing in the NP size distribution. The addition of the ZnO cupping layer led to a narrower NP size distribution, as well as to a decrease in the number and the size of large submicroscopic particles in the samples.

The optical and structural properties of the samples with Ag NPs in the ZnO matrix were shown to be determined by the diffusion of silver passing through the ZnO cupping layer during annealing. The ZnO cupping layer and its thickness affect the above process.

References

1. Jiang J, Wang X, Li S, Ding F, Li N, Meng S, Li R, Qi J, Liu Q, Liu GL. Plasmonic nanoarrays for ultrasensitive bio-sensing. *Nanophotonics*. 2018;7(9): 1517–1531.
2. Barizuddin S, Bok S, Gangopadhyay S. Plasmonic sensors for disease detection-a review. *Journal of Nanomedicine and Nanotechnology*. 2016;7(3): 1000373.
3. Varghese AK, Tamil PP, Rugmini R, Shiva PM, Kamakshi K, Sekhar KC. Green synthesized Ag nanoparticles for bio-sensing and photocatalytic applications. *ACS Omega*. 2020;5(22): 13123–13129.
4. Ross MB, Mirkin CA, Schatz GC. Optical properties of one-, two-, and three-dimensional arrays of plasmonic nanostructures. *Journal of Physical Chemistry C*. 2016;120(2): 816–830.
5. Wang W, Qi L. Light management with patterned micro-and nanostructure arrays for photocatalysis, photovoltaics, and optoelectronic and optical devices. *Advanced Functional Materials*. 2019;29(25): 1807275.
6. Chaldyshev VV, Kolesnikova AL, Bert NA, Romanov AE. Investigation of dislocation loops with As-Sb nanoclusters in GaAs. *Journal of Applied Physics*. 2005;97: 024309.
7. Chaldyshev VV, Bert NA, Kolesnikova AL, Romanov AE. Stress Relaxation Scenario for Buried Quantum Dots. *Physical Review B*. 2009;79(23): 233304.
8. Gutkin MY, Smirnov AM. Initial stages of misfit stress relaxation in composite nanostructures through generation of rectangular prismatic dislocation loops. *Acta Materialia*. 2015;88: 91–101.
9. Gutkin MY, Krasnitckii SA, Smirnov AM, Kolesnikova AL, Romanov AE. Dislocation loops in solid and hollow semiconductor and metal nanoheterostructures. *Physics of the Solid State*. 2015;57: 1177–1182.
10. Mizuno A, Ono A. Static and dynamic tuning of surface plasmon resonance by controlling interparticle distance in arrays of Au nanoparticles. *Applied Surface Science*. 2019;480: 846–850.
11. Yilmaz M, Senlik E, Biskin E, Yavuz MS, Tamer U, Demirel G. Combining 3-D plasmonic gold nanorod arrays with colloidal nanoparticles as a versatile concept for reliable, sensitive, and selective molecular detection by SERS. *Physical Chemistry Chemical Physics*. 2014;16(12): 5563–5570.
12. Liu B, Yao X, Chen S, Lin H, Yang Z, Liu S, Ren B. Large-area hybrid plasmonic optical cavity (HPOC) substrates for surface-enhanced Raman spectroscopy. *Advanced Functional Materials*. 2018;28(43): 1802263.
13. Wang Z, Ai B, Möhwald H, Zhang G. Colloidal lithography meets plasmonic nanochemistry. *Advanced Optical Materials*. 2018;6(18): 1800402.
14. Bagheri S, Strohfeldt N, Sterl F, Berrier A, Tittl A, Giessen H. Large-area low-cost

plasmonic perfect absorber chemical sensor fabricated by laser interference lithography. *ACS Sensors*. 2016;1(9): 1148–1154.

15. Jeong HH, Mark AG, Lee TC, Son K, Chen W, Alarcón-Correa M, Kim I, Schütz G, Fischer P. Selectable Nanopattern Arrays for Nanolithographic Imprint and Etch-Mask Applications. *Advanced Science*. 2015;2(7): 1500016.

16. Terekhin VV, Dement'eva OV, Rudoy VM. Formation of ordered nanoparticle assemblies by block copolymer lithography methods. *Russian Chemical Reviews*. 2011;80(5): 453.

17. Saifullina IR, Chiganova GA, Karpov SV, Slabko VV. Preparation of composite films with silver nanoparticles and their fractal aggregates in a polymeric matrix. *Russian Journal of Applied Chemistry*. 2006;79: 1639–1642.

18. Kasani S, Curtin K, Wu N. A review of 2D and 3D plasmonic nanostructure array patterns: fabrication, light management and sensing applications. *Nanophotonics*. 2019;8(12): 2065–2089.

19. Chentsova IE, Dubovik VI, Kovivchak VS. Synthesis of silver nanoparticles by thermal annealing of thin films. *Herald of Omsk University*. 2012;2: 110–114.

20. Ignat'ev AI, Nashchekin AV, Nevedomskii VN, Podsvirov OA, Sidorov AI, Solov'ev AP, Usov OA. Formation of Silver Nanoparticles in Photothermorefractive Glasses during Electron Irradiation. *Technical Physics*. 2011;56(5): 662.

21. Stepanov AL, Popok VN, Hole DE, Bukharaev AA. Interaction of high-power laser pulses with glasses containing implanted metallic nanoparticles. *Physics of the Solid State*. 2001;43: 2192–2198.

22. Gromov DG, Pyatilova OV, Bulyarskii SV, Belov AN, Raskin AA. Specific features of the formation of arrays of silver clusters from a thin film on a SiO₂ surface. *Physics of the Solid State*. 2013;55: 619–623.

23. Ruffino F, Torrisi V, Marletta G, Grimaldi MG. Growth morphology of nanoscale sputter-deposited Au films on amorphous soft polymeric substrates. *Applied Physics A*. 2011;103: 939–949.

24. Ranjbar M, Kameli P, Salamati H. Coalescence threshold temperature in Ag nanoisland growth by pulsed laser deposition. *Materials Physics and Mechanics*. 2013;17(1): 21–28.

25. Sokura LA, Shirshneva-Vaschenko EV, Kirilenko DA, Snezhnaia ZhG, Shirshnev PS, Romanov AE. Electron-microscopy study of ordered silver nanoparticles synthesized in a ZnO:Al polycrystalline film. *Journal of Physics: Conference Series*. 2019;1410(1): 012170.

26. Shirshneva-Vaschenko EV, Sokura LA, Baidakova MV, Yagovkina MA, Snezhnaia ZhG, Shirshnev PS, Romanov AE. Study of the influence of the ZnO:Al polycrystalline film morphology on the silver nanoparticles formation. *Journal of Physics: Conference Series*. 2019;1400(5): 055026.

27. Sokura LA, Snezhnaia ZhG, Nevedomskiy VN, Shirshneva-Vaschenko EV, Romanov AE. Ordering mechanism of silver nanoparticles synthesized in a ZnO:Al polycrystalline film by sol gel method. *Journal of Physics: Conference Series*. 2020;1695(1): 012034.

28. Rao DVS, Muraleedharan K, Humphreys CJ. TEM specimen preparation techniques. *Microscopy: Science, Technology, Applications and Education*. 2011;2: 1232–1244.

29. Denisov NM, Chubenko EB, Bondarenko VP, Borisenko VE. Optical Properties of Multilayered Sol–Gel Zinc-Oxide Films. *Semiconductors*. 2018;52(6): 723–728.

30. Muzalev PA, Kosobudskii ID, Kul'batskii DM, Ushakov NM, Podvigalkin VY. Synthesis, structure, and properties of silver nanocomposite materials with poly (hydroxyethyl methacrylate) matrix. *Russian Journal of Applied Chemistry*. 2011;84: 666–669.

31. Shirshneva-Vaschenko EV, Sosnin IM, Nuryev RK, Gladskikh IA, Liashenko TG, Bougrov VE, Romanov AE. Electrical and optical properties of transparent conducting ZnO: Al/AgNP multilayer films. *Materials Physics and Mechanics*. 2016;29(2): 145–149.

32. Kreibig U, Vollmer M. *Optical properties of metal clusters*. Berlin: Springer; 1995.
33. Ross MB, Blaber MG, Schatz GC. Using nanoscale and mesoscale anisotropy to engineer the optical response of three-dimensional plasmonic metamaterials. *Nature Communications*. 2014;5(1): 4090.
34. Sokura LA, Ryabkova EA, Kirilenko DA, Shirshneva-Vaschenko EV. Structural and Optical Properties of Silver Nanoparticles In Situ Synthesized in ZnO Film by Sol–Gel Method. *Reviews on Advanced Materials and Technologies*. 2021;3(4): 29–33.

THE AUTHORS

Sokura L.A. 

e-mail: sokuraliliy@mail.ru

Kremleva A.V. 

e-mail: avkremleva@itmo.ru

Romanov A.E. 

e-mail: alexey.romanov@niuitmo.ru